OPEN-LOOP AND FEEDBACK PECTORAL FIN CONTROL OF BIOROBOTIC AUV

Sahjendra N. Singh and Aditya Simha

Department of Electrical & Computer Engineering,
University of Nevada, Las Vegas, NV. 89154-4026
Email: sahaj@ee.unlv.edu; aditya@egr.unlv.edu

Abstract

The paper treats the question of dive plane control of biorobotic undersea vehicles (AUVs) using oscillating pectoral fins. The forces and moment produced by the pectoral fins are complicated functions of the modes of oscillations (lead-lag, feathering and flapping) as well as the oscillation parameters such as the frequency and amplitude of oscillation, phase angle and bias angle. Experimental results indicate that the fin forces are mostly periodic. We present control systems for the dive plane maneuver using the periodic forces and moments of the fins. Two kinds of control laws are derived. The first control law is for the open-loop synthesis. Here the Fourier coefficients of the periodic force and moment play a key role in the controller design. The open-loop controller assumes a fixed mode of oscillation of the fins. A set of Fourier coefficients associated with the fin force are obtained for a finite time transition of the vehicle to any desired depth. By a choice of sufficient number of harmonics in the fin oscillation, a large set of Fourier coefficients for maneuver are obtained. The second design provides a feedback control system and uses the periodically updated bias angle as the control input. The bias angle switches every $n_0 T_0$ second where T_0 is the fundamental period of the fin force and moment and n_0 is a positive integer. The design uses discretized model and integral feedback for precision in depth control. Simulation results for both the open-loop and closed-loop control systems are present. These results show that the pectoral fins can accomplish rapid and precise control in the dive plane.

1. Introduction

Fishes and aquatic mammals are marvelous swimmers and have the ability to perform swift and complex maneuvers employing oscillating fins [1, 2]. This has motivated researchers to design flapping foils for propulsion and control of biorobotic autonomous undersea vehicles(AUVs) [3-6]. These biologically-inspired control surfaces can provide AUVs with greater maneuverability as well as efficient propulsion. Studies have been carried out on fish morphology, locomotion, and application of biologically-inspired control surfaces to rigid bodies [3, 6-8]. Considerable effort has been made to measure the forces and moments produced by oscillating fins in laboratory experiments [4-6, 8-11]. It has been observed that pectoral fins undergoing a combination of lead-lag, feathering and flapping motion have the ability to produce large lift, side force and thrust which can be used for the control and propulsion of AUVs [8-11]. In several studies, computational methods have been also used to obtain forces and moments of flapping and pitching foils [12-14]. These experimental and numerical results provide forces produced by the fins for only a set of motion patterns of oscillating fins. An analytical representation of the unsteady hydrodynamics of oscillating foil have been obtained using Theodorsen's theory [15]. Finite dimensional models are extremely interesting from the point of view of control system design. Because analytical representation of forces is extremely complicated, neural networks and fuzzy controllers have been suggested for controller design [9-11]. Of course, the designer must have sufficient knowledge of the effect of fin forces on the vehicle to develop rule-based logic for the control of AUVs. It appears from literature, that only little theoretical research has been done to design control systems using pectoral fins.

The contribution of this paper lies in the design of control systems for the dive plane maneuvering of biorobotic AUVs using pectoral fins. These pectoral fins produce variety of periodic forces and moments which have wide range of harmonic functions depending on the oscillation mode and oscillation parameters of the fins. It is essential to capture their basic features which simplifies controller design. For this purpose, characterization of these periodic forces using Fourier series is very attractive. These Fourier coefficients play an important role in the design of the control systems in this paper. Two kinds of control laws (an open-loop and a closed-loop) for maneuvering are derived. For the open-loop control, an analytical solution for the Fourier-coefficients is derived for a given maneuver. The derived coefficients in turn determine the required fin forces and moments for the maneuver of the vehicle. It is seen that for a given maneuver there exist multiple solutions for the pectoral force and moment. This flexibility can be exploited to satisfy certain given performance criteria. The second control system uses state variable feedback for synthesis. For the closed-loop control, the bias angle is utilized as the control input. For the purpose of control, the bias angle is switched to new values at the chosen sampling instants which are integer multiple of the fundamental time period of the fin force and moment. An integral feedback is included in the control law for the precise depth control. In the open-loop control scheme, the pectoral fins complete the maneuver by operating in a fixed oscillation mode with constant oscillation parameters. However, for each maneuver one needs to compute the motion pattern separately. Simulation results using the open-loop and closed-loop control systems are obtained for the dive plane control.

The organization of the paper is as follows. Section 2 presents the dive plane dynamics while Section 3 considers the derivation of an open-loop control law. Simulation results for the same are presented in Section 4. The derivation of a closed-loop control law is considered in Section 5 and numerical results for the closed-loop depth control are shown in Section 6.

2. Dive Plane Dynamics

Let the vehicle be moving in the dive plane ($X_I - Z_I$ plane) where $O_I X_I Z_I$ is an inertial coordinate system (Fig. 1). $O_B X_B Z_B$ is a body fixed coordinate system; X_B is in the forward direction, and Z_B points down. The heave and pitch equations of motion are described by coupled nonlinear differential equations.

In the moving coordinate frame $O_B X_B Z_B$ fixed at the vehicle's geometric center, the equations of motion for neutrally buoyant vehicle are given by

$$
\begin{gathered}
m(\dot{w} - uq - z_G q^2 - x_G \dot{q}) = \\
0.5\rho l^4 z'_{\dot{q}} \dot{q} l + 0.5\rho l^3 z'_{\dot{w}} \dot{w} + z'_q qu \\
+0.5\rho l^2 z'_w wu + f_p \\
I_y \dot{q} + m z_G(\dot{u} + wq) - m x_G(\dot{w} - uq) = \\
0.5\rho l^5 M'_{\dot{q}} \dot{q} + 0.5\rho l^4 M'_{\dot{w}} \dot{w} + M'_q qu \\
+0.5\rho l^3 M'_w wu - x_{GB} W \cos\theta - z_{GB} W \sin\theta + m_p \\
\dot{z} = -u \sin\theta + w \cos\theta \qquad (1)
\end{gathered}
$$

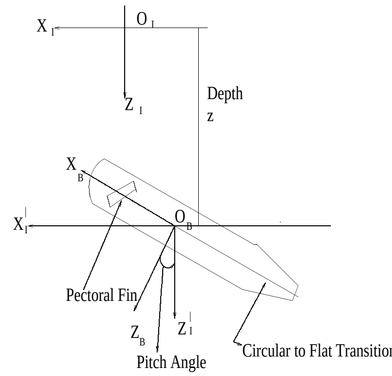

Figure 1: Schematic of the AUV

where θ is the pitch angle, $q = \dot{\theta}$, $x_{GB} = x_G - x_B$, $Z_{GB} = z_G - z_B$, $l=$ body length, $\rho =$ density, w is the velocity along the Z_B-axis, and z is the depth. f_p and m_p denote the force and moment produced by the pectoral fins. Here X_G, Z_G and X_B, Z_B are the coordinates of the center of gravity and the center of buoyancy, respectively. It is assumed that O_B is at the center of buoyancy and the forward velocity is held steady ($u = U$) by a control mechanism.

In this study, only small maneuvers of the vehicle are considered. As such linearizing the equations of motion about $w = 0, q = 0, z = 0$ and $\theta = 0$, one obtains

$$
\begin{bmatrix} m - z_{\dot{w}} & -m x_G - z_{\dot{q}} & 0 \\ -m x_G - M_{\dot{w}} & I_y - M_{\dot{q}} & 0 \\ 0 & 0 & 1 \end{bmatrix} \begin{bmatrix} \dot{w} \\ \dot{q} \\ \dot{z} \end{bmatrix} =
$$

$$
\begin{bmatrix} z_w U & z_q + mU & 0 \\ M_w U & M_q - m x_G U & 0 \\ 1 & 0 & 0 \end{bmatrix} \begin{bmatrix} w \\ q \\ z \end{bmatrix}
$$

$$
+ \begin{bmatrix} 0 \\ -Z_{GB} W \\ -U \end{bmatrix} \theta + \begin{bmatrix} f_p \\ m_p \\ 0 \end{bmatrix} \qquad (2)
$$

where $x_{GB} = 0$. Here we have introduced new parameters ($z_{\dot{w}}$, $M_{\dot{q}}$, etc.) which are proportional to the nondimensionalized (primed) hydrodynamic coefficients. Defining the state vector $x = (w, q, z, \theta)^T \in R^4$ and solving (2), one obtains a state variable representation of the form

$$
\dot{x} = Ax + B \begin{bmatrix} f_p \\ m_p \end{bmatrix} \qquad (3)
$$

for appropriate matrices $A \in R^{4\times 4}$ and $B \in R^{4\times 2}$.

The force and moment produced by the oscillatory pectoral fins are quite complex and depend on the motion pattern of the fins. In the most general case the pectoral fins can have lead-lag, feathering and flapping motion. The force and moment also depend on the oscillation parameters such as the frequency and amplitude of oscillations, the bias angle, and the phase angle which can be independently varied and thus can be treated as control inputs. Experimental results indicate that the oscillatory foils produce periodic forces in the steady state. Although, as indicated above, one can have several independent control inputs, it is assumed here that the pectoral fins have flapping and pitching motion given by

$$h(t) = \sum_{n=1}^{N} h_{on} \cos(nw_f t + \nu_n) + \beta_h$$

$$\psi(t) = \sum_{n=1}^{N} \psi_{on} \cos(nw_f t + \nu_n) + \beta_\psi \quad (4)$$

where w_f, h_{on}, ψ_{on} are the frequency and amplitudes of oscillations and β_h and β_ψ are the biases which can be used as the control inputs. The periodic force and moment generated by the fins are nonlinear functions of these control inputs. Since $f_p(t)$ and $m_p(t)$ are periodic functions, they can be represented by the Fourier series

$$f_p = \sum_{n=0}^{M} (f_{sn} \sin(nw_f t) + f_{cn} \cos(nw_f t))$$

$$m_p = \sum_{n=0}^{M} (m_{sn} \sin(nw_f t) + m_{cn} \cos(nw_f t)) \quad (5)$$

where it is assumed that the fin produces dominant M harmonically related components and the harmonics of higher frequencies are negligible. The Fourier coefficients f_{ij} and m_{ij} capture the characteristics of the time-varying signals $f_p(t)$ and $m_p(t)$ and play a key role in the design of control systems for maneuvering.

We are interested in the design of an open-loop and a closed-loop (feedback) control systems for the dive plane control of the vehicle. This way the AUV can be maneuvered to operate at different depths on command.

3. Open-loop Control System

In this section, first the design of the open-loop controller is considered. Let the initial condition be $x(0) = x_0$ and suppose that it is desired to steer the vehicle to the terminal state $x^* = (0, 0, z^*, 0)^T$, where z^* denotes the desired input. For simplicity in presentation, we assume that only the first and second harmonics are present in (5). Then (5) gives

$$f_p = \begin{bmatrix} 1 & \sin w_f t & \cos w_f t & \sin 2w_f t & \cos 2w_f t \end{bmatrix} p_f$$
$$\doteq \phi^T(t) p_f$$
$$m_p = \phi^T(t) p_m \quad (6)$$

where the vector function $\phi(t) \in R^5$ is

$$\phi^T = \begin{bmatrix} 1 & \sin w_f t & \cos w_f t & \sin 2w_f t & \cos 2w_f t \end{bmatrix}$$

and the vector of the Fourier coefficients are

$$p_f = \begin{bmatrix} f_{c0} & f_{s1} & f_{c1} & f_{s2} & f_{c2} \end{bmatrix}^T \in R^5$$

$$p_m = \begin{bmatrix} m_{c0} & m_{s1} & m_{c1} & m_{s2} & m_{c2} \end{bmatrix}^T \in R^5$$

are the constant parameters. Now for steering the vehicle from the initial condition x_0 to x^*, we shall find appropriate values of the vectors p_f and p_m associated with the fin force and moment.

The solution of (3) and (6) can be written as

$$x(t) = e^{At} x_0 + \int_0^t e^{A(t-\tau)} B\Phi(\tau) p d\tau \quad (7)$$

where $p = (p_f^T, p_m^T)^T \in R^{10}$ is a constant vector and

$$\Phi(t) = \begin{bmatrix} \phi^T(t) & 0 \\ 0 & \phi^T(t) \end{bmatrix} \in R^{2\times 10}$$

and 0 denotes null matrices of appropriate dimensions.

Define

$$X_0(t) = e^{At} x_0$$

$$Z(t) = \int_0^t e^{A(t-\tau)} B\Phi(\tau) d\tau \quad (8)$$

Then $X_0(t) \in R^4$ and $Z(t) \in R^{4\times 10}$ can be obtained by solving the differential equations

$$\dot{X}_0(t) = AX_0(t), X_0(0) = x_0,$$

$$\dot{Z}(t) = AZ(t) + B\Phi(t), Z(0) = 0 \quad (9)$$

For the transfer of x_0 to x^* at the instant $t^* > 0$, using (7) and (8), one must have

$$x^* = X_0(t^*) + Z(t^*)p \quad (10)$$

For the existence of solution of (10), $x^* - X_0(t^*)$ must be in the range space of $Z(t^*)$. Since x_0 is arbitrary, (10) can be solved for p if rank $\{Z(t^*)\} = 4$. Noting that (10) does not have a unique solution, an optimal value of p can be obtained by minimizing an appropriate quadratic function

$$J = p^T W p$$

where W is a symmetric positive definitive weighting matrix. By the choice of W, one can obtain suitable values of the vector p. Then the unique solution for p obtained by minimizing J can be shown to be

$$p^* = W^{-1} Z^T(t^*)(Z(t^*)W^{-1}Z^T(t^*))^{-1}(x^* - X_0(t^*)) \tag{11}$$

One notes that a general solution of (10) can be written as

$$p = p^* + q \tag{12}$$

where $q \in N(Z(t^*))$, the null space of $Z(t^*)$. Indeed the pectoral fin forces and moment for which the Fourier coefficients q belong to the null space of $Z(t^*)$ do not contribute to the transfer of x_0 to x^*.

To this end, it is appropriate to discuss, the question related to the synthesis of the desired control law. It is pointed out that the rank of $Z(t^*)$ depends not only on the pectoral fin oscillation mode and oscillation parameters, but also on the choice of the transfer interval $[0, t^*]$. Because, the forcing function in the Z-dynamics is $\Phi(t)$ consisting of sinusoidal signals, $Z(t)$ is sinusoidal and the determinant Δ of $Z(t)Z^T(t)$ is is an oscillatory function of time. One can select any value of t^*, such that $\Delta(t^*)$ yields a feasible p^* associated with the pectoral fin motion. Since, pectoral fins can have a variety of motions, they have the capability to generate forces and moments yielding a set of p large enough which contains p^*. The Fourier coefficients are functions of the oscillation parameters and belong to certain bounded intervals. As such, one can use constrained optimization algorithms to obtain solution of (10) with inequality constraints on the Fourier coefficients.

According to (5), the dimension of the design-parameter vector $p = (p_f^T, p_m^T)^T$ increases if additional sinusoidal components in the fin force and moment are included. Fin forces consisting of larger number of harmonic terms by the choice of M in (4) provide flexibility in satisfying (10) which can be exploited to satisfy certain response characteristics of the dive-plane control system. It is also pointed out that the design approach presented in this section is equally applicable if the fin motion is not periodic.

4. Numerical results: Open-loop Control

In this section simulation results for the system (3) with the open-loop control law (6) and (12) using $p = p^*$ with $W = I$ are presented (I denotes an identity matrix). The model parameters for simulation of the vehicle are taken from [7]. It is assumed that the vehicle is initially moving horizontally at a constant speed U = 3 (m/s) and the initial condition is $x(0) = (0, 0, 0, 0)^T$. The desired state at t^* is selected as $x^* = (0, 0, z^*, 0)^T$. That is, one would like to maneuver the vehicle such that at $t = t^*$, the vehicle dives down to a depth of z^* and subsequently moves horizontally.

Case 4.1: Open-loop control: $z^* = 4$ (m), $t^* = 20$ (s), $w_f = 40$ (rad/s)

It is desired to maneuver in $t^* = 20$ seconds and z^* is taken to be 4 (m). The frequency w_f is chosen as $w_f = 40$ (rad/sec). Thus f_p contains sinusoidal terms of frequencies 40 and 80 (rad/s). Of course it is assumed that the fin motion in (4) is suitably chosen to yield fin force of the form indicated. Although the control system of Section 3 is applicable to any general case, for the purpose of illustration, we assumed here a restricted case in which $m_p = 0.25 f_p$, that is f_p and m_p are linearly related. Such situations do arise for certain oscillation patters of the fins. It is noted that by the choice of linearly related moment and force, one has fewer elements in the control parameter vector p ($p = p_f \in R^5$, $p_m = 0.25 p_f$) to satisfy (10) for maneuvering the vehicle; however, it is found that in spite of this limitation, several solutions for p still exist and maneuver can be completed.

The simulated responses are as shown in Figs. 2 and 3. The plot of the determinant $\Delta(t)$ of $(Z(t)Z(t)^T)$ is shown in the Fig. 2. It is seen that $\Delta(t)$ is oscillatory and for the chosen w_f, one can select any $t^* > 12$ (sec) for maneuvering as long as $\Delta(t^*) \neq 0$.

Fig. 3 shows smooth convergence of the depth trajectory to the desired value (4 (m)) in the chosen time interval of 20 seconds. During this interval of time one observes an oscillation of extremely small amplitude superimposed on the mean pitch angle trajectory. The pitch rate and pitch angles are also have oscillatory motion. However, it is pointed out that the initial state $x(0) = 0$ is precisely steered to the chosen state $x^* = (0, 0, 4, 0)^T$ at $t = 20$ (sec). Indeed if the fin force and moment are set to zero beyond 20 (sec), the vehicle continues to move along the horizontal path (The plots beyond 20 (sec) are not shown here). Oscillatory fin force f_p (shown only over $t \in [0, 1.5]$ (sec) for clarity) of magnitude less than 50 (N) is required for the maneuver. The pitch angle swings between -5 and 0 degrees. The maximum magnitude of the velocity w remains within 0.08 (m/s) which is quite small. The pitch rate is

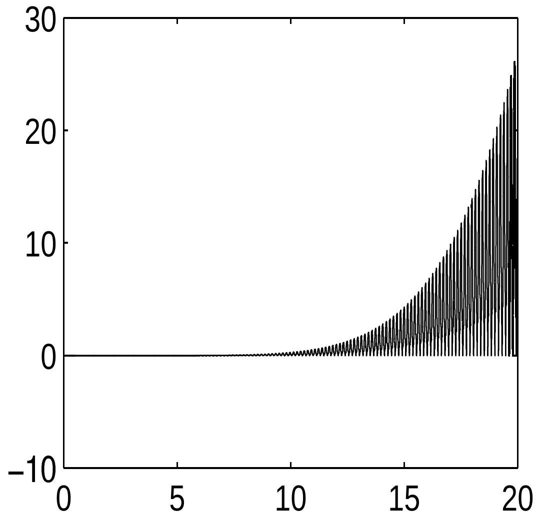

Figure 2: Open-loop control: Determinant of $Z(t)Z^T(t)$

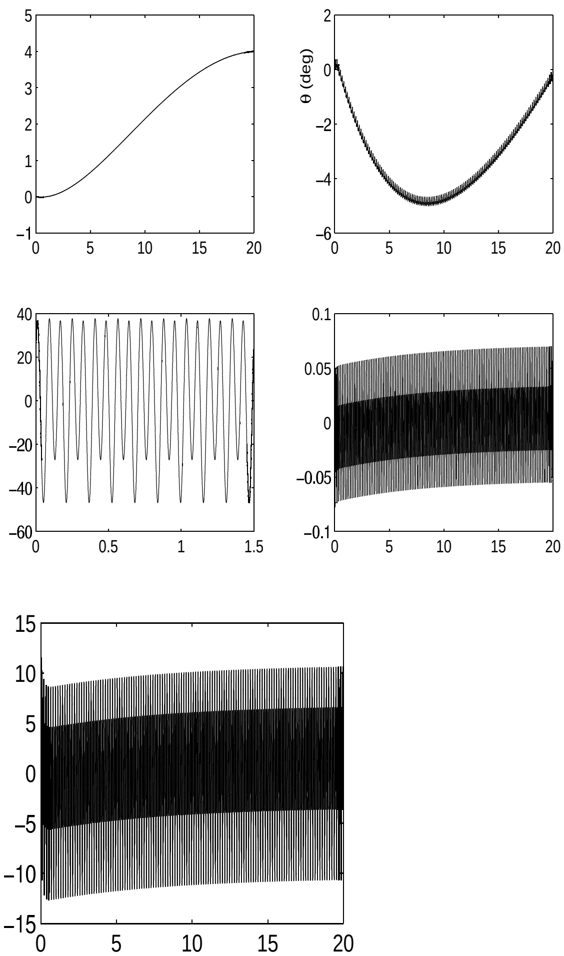

Figure 3: Open-loop control: $z^* = 4$(m), $w_f = 40$ (rad/sec)

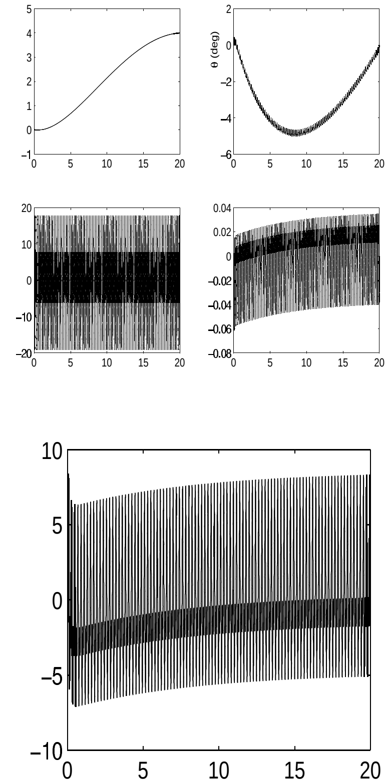

Figure 4: Open-loop control: $z^* = 4$(m), $w_f = 30$ (rad/sec)

also small (less than 15 (deg/sec). We observe small nonzero average values of the pitch rate and the velocity w.

Case 4.2 Open-loop Control: $z^* = 4$ (m), $t^* = 20$ (s), $w_f = 30$ (rad/s).

Simulation is done using a lower value of w_f but the remaining conditions of Case 4.1 are retained. The responses are shown in Fig. 4.

We observe that the vehicle smoothly attains the desired depth as well as the terminal state. at 20 seconds. The pitch angle is between -5 and 0 degrees. The maximum magnitude of the normal force is less than 20 N. The velocity stays between -0.06 to about 0.035 (m/s). It is seen that for lower frequency of oscillation the magnitude of the normal force is smaller. Of course, one can obtain different normal force history for the maneuver by selecting the weighting matrix $W \neq I$.

Case 4.3 Open-loop Control: $z^* = 2$ (m), $t^* = 20$ (s), $w_f = 30$ (rad/s).

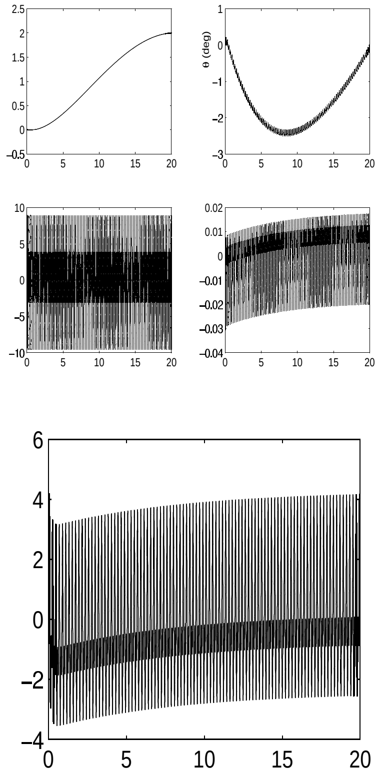

Figure 5: Open-loop control: $z^* = 2$(m), $w_f = 30$ (rad/sec)

The simulation is done by retaining the conditions of Case 4.2. But a smaller terminal depth z^* = 2 (m) for control is chosen. The responses are as shown in Fig. 5.

The desired depth and terminal state are reached at 20 seconds. The pitch angle varies between -2.5 and 0 degrees. The normal force is less than 10 N which is almost half of that required for Case 4.2. The maximum velocity is only slightly over 0.03 (m/sec) and the pitch rate is less than 4.5 (deg/sec). Thus it is seen that smaller commands for maneuver can be chosen to reduce the magnitudes of state trajectories and the control input in the transient period.

5. Closed-loop Control Design

In this section, the design of a feedback dive-plane control law is considered. Unlike the open-loop control system of the previous section, in which pectoral fins have a fixed motion pattern, here it is assumed that there are control variables which can be altered periodically. Although, one can chose a variety of oscillation parameters such as the amplitudes and frequency of oscillation and phase and bias angles, for simplicity in presentation, we assume that only the bias angles $\beta = \beta_\psi$ is varied periodically and $\beta_h = 0$ and the remaining oscillation parameters are constant.

It has been experimentally shown that the mean value of the normal force and the pitching moment varies almost linearly with β [5] and the amplitude of fin force and moment are functions of β. Expanding the fin force and moment in a Taylor series about $\beta = 0$ gives:

$$f_p(t, \beta) = f_p(t, 0) + \frac{\partial f_p}{\partial \beta}(t, 0)\beta + O(\beta^2)$$

$$m_p(t, \beta) = m_p(t, 0) + \frac{\partial m_p}{\partial \beta}(t, 0)\beta + O(\beta^2) \quad (13)$$

where $O(\beta^2)$ denotes higher order terms. We assume here that for a fixed $\beta \in R$, $f_p(t + T_0, \beta) = f_p(t, \beta)$ and $m_p(t + T_0, \beta) = m_p(t, \beta)$, $t > 0$ (T_0 denotes the fundamental period). Then the partial derivatives of f_p and m_p with respect to β are also periodic functions of time. Then using (5) and (13), one can approximately express f_p and m_p as

$$f_p = \sum_{n=0}^{M} f_{sn}(0) \sin nw_f t + f_{cn}(0) \cos nw_f t +$$

$$\sum_{n=0}^{M} \left(\frac{\partial f_{Sn}}{\partial \beta}(0) \sin nw_f t + \frac{\partial f_{cn}}{\partial \beta}(0) \cos nw_f t\right)\beta$$

$$m_p = \sum_{n=0}^{M} m_{sn}(0) \sin nw_f t + m_{cn}(0) \cos nw_f t +$$

$$\sum_{n=0}^{M} \left(\frac{\partial M_{sn}}{\partial \beta}(0) \sin nw_f t + \frac{\partial M_{cn}}{\partial \beta}(0) \cos nw_f t\right)\beta \quad (14)$$

where $O(\beta^2)$ terms are ignored in the series expansion. For simplicity in presentation, we assumed that $M = 2$ similar to Section 3.

We define

$$f_a = (f_{c0}(0), f_{s1}(0), f_{c1}(0), f_{s2}(0), f_{c2}(0))^T$$

$$f_b = \left(\frac{\partial f_{c0}}{\partial \beta}(0), \frac{\partial f_{s1}}{\partial \beta}(0), \frac{\partial f_{c1}}{\partial \beta}(0), \frac{\partial f_{s2}}{\partial \beta}(0), \frac{\partial f_{c2}}{\partial \beta}(0)\right)^T$$

$$m_a = (m_{c0}(0), m_{s1}(0), m_{c1}(0), m_{s2}(0), m_{c2}(0))^T$$

$$m_b = \left(\frac{\partial m_{c0}}{\partial \beta}(0), \frac{\partial m_{s1}}{\partial \beta}(0), \frac{\partial m_{c1}}{\partial \beta}(0), \frac{\partial m_{s2}}{\partial \beta}(0), \frac{\partial m_{c2}}{\partial \beta}(0)\right)^T \quad (15)$$

Then using (14) and (15), we get

$$f_p(t) = \phi^T (f_a + \beta f_b)$$

$$m_p(t) = \phi^T(m_a + \beta m_b) \tag{16}$$

and the dive plane dynamics take the form

$$\dot{x} = Ax + B\Phi(t)f_c + B\Phi(t)f_v\beta \tag{17}$$

where

$$f_c = (f_a^T, m_a^T) \in R^{10} \tag{18}$$

$$f_v = (f_b^T, m_b^T) \in R^{10}$$

For the purpose of control, the bias angle is periodically changed at a sampling interval of T^* where T^* is an integer multiple of the period T_0, i.e., $T^* = n_0 T_0$, where n_0 is a positive integer. This way one switches the bias angle at an uniform rate of T^* seconds at the end of n_0 cycles.

For the derivation of the control law, the transients introduced due to switching are ignored in this study. Since the bias is changed periodically, it will be convenient to express the continuous-time system (17) as a discrete-time system. The function $\beta(t)$ now has piecewise constant values β_k for $t \in [kT^*, (k+1)T^*), k = 0, 1, 2......$ The solution of (17) is given by

$$x(t) = e^{A(t-t_0)}x(t_0) + \int_{t_0}^{t} e^{A(t-t_0)}B\Phi(\tau)[f_c + f_v\beta(\tau)]d\tau \tag{19}$$

Taking $t_0 = kT^*$, and $t = (k+1)T^*$, one has

$$x[(k+1)T^*] = e^{AT^*}x(kT^*) +$$

$$\int_{kT^*}^{(k+1)T^*} e^{A[(k+1)T^* - \tau]}B\Phi(\tau)[f_c + f_v\beta_k]d\tau \tag{20}$$

since $\beta(t) = \beta_k$, $t \in [kT^*, (k+1)T^*)$

Let $(k+1)T^* - \tau = s$. Then noting that

$$\Phi((k+1)T^* - s) = \Phi(-s) \tag{21}$$

(20) gives

$$x[(k+1)T^*] = e^{AT^*}x(kT^*) +$$

$$\int_0^{T^*} e^{As}B\Phi(-s)[f_c + f_v\beta_k]ds$$

$$\doteq A_d x(kT^*) + B_d[f_c + f_v\beta_k] \tag{22}$$

where $A_d = e^{AT^*}$ and $B_d = \int_0^{T^*} e^{As}B\Phi(-s)ds$. For the precise depth control, it is desirable to include a feedback term in the control law which is proportional to the integral of the depth tracking error. For this, a new state variable x_s is introduced which satisfies

$$x_s[(k+1)T^*] = z^* - y(kT^*) + x_s(kT^*) \tag{23}$$

where $z^* - y(kT^*)$ is the tracking error,

$$y(kT^*) = z(kT^*) = Cx(kT^*) \tag{24}$$

and $C = [0, 0, 1, 0]$.

Defining the augmented state vector x_a as

$$x_a = (x^T, x_s)^T \in R^5$$

the system (22) and (23) is written as

$$x_a[(k+1)T^*] = \begin{bmatrix} A_d & 0 \\ -C & 1 \end{bmatrix} \begin{bmatrix} x(kT^*) \\ x_s(kT^*) \end{bmatrix} +$$

$$\begin{bmatrix} B_d f_v \\ 0 \end{bmatrix} \beta_k + \begin{bmatrix} B_d f_c \\ z^* \end{bmatrix}$$

$$\doteq A_a x_a(kT^*) + B_a\beta_k + d_a \tag{25}$$

where the constant matrices A_a, B_a and d_a are defined in (25).

The control of the system (25) can be accomplished by following the servomechanism design approach in which d_a is treated as a constant disturbance input. The design is easily completed by computing a feedback control law of the form

$$\beta(kT^*) = -Kx_a(kT^*), k = 0, 1, 2, ... \tag{26}$$

where K is a constant row vector such that the closed-loop matrix

$$A_c = (A_a - B_a K)$$

is stable. It is well known that that one can assign the eigenvalues of A_c arbitrarily if (A_a, B_a) is controllable [16-18]. For the discrete-time system, this implies that one must choose K such that the eigenvalues of A_c are strictly within a unit disk in the complex plane.

In this study, an appropriate value of K is obtained by using the linear quadratic optimal control theory. For this one chooses a performance index of the form

$$J_o = \sum_{k=0}^{\infty} x_a^T(kT^*)Qx_a(kT^*) + \beta_k^2\mu \tag{27}$$

where Q is a positive definite symmetric matrix and $\mu > 0$. The optimal control law is obtained by minimizing J_o for the system

$$x_a[(k+1)T^*] = A_a x(kT^*) + B_a\beta_k \tag{28}$$

The system (28) is obtained by setting $d_a = 0$ in (25). The feedback matrix K is obtained by solving the discrete Ricaati equation [18]

$$P = Q + A_a^T P A_a - A_a^T P B_a(\mu + B_a^T P B_a)B_a^T P A_a \tag{29}$$

and then setting the feedback matrix as

$$K = -(\mu + B_a^T P B_a)^{-1} B_a^T P A_a \qquad (30)$$

The choice of the weighting matrix Q and the parameter μ is made to obtain desirable responses and the convergence of the tracking error to zero.

To this end, a discussion of the two designed control systems is appropriate. We note that the open-loop controller of the previous section does not require any change in the motion pattern of the pectoral fins. For the open-loop control scheme, the Fourier coefficient associated with fin force and moment are determined. It is essential that these coefficients lie in the feasible parameter set Ω obtained by certain choice of motion pattern and oscillation parameters of the pectoral fins. For the feedback control system designed in this section, the bias angle is periodically varied and kept constant over the selected sampling period $T^* = n_0 T_0$. The pectoral fin must produce force and moment such that the controllability condition is satisfied. The choice of the sampling period also provides flexibility in meeting the controllability condition. The synthesis of the feedback control law requires measurement of all the state variables, and switching of the bias angles by the actuator. However closed-loop system can provide robustness to parameter uncertainty compared to the open-loop control system. The closed-loop system provides asymptotic regulation of the tracking error. But open-loop control law can complete maneuver in a finite specified time. As such one can use a dual mode control synthesis for depth control in which one first uses the open-loop control law and then switches to the feedback law for precise regulation in the vicinity of the terminal state.

6. Simulation Results: Closed-loop Control

In this section, the feedback discrete control law (26) is simulated. For the optimal control law design, the performance index J_o with $Q = diag(1, 1500, 1, 1000, 1)$ and $\mu = 400$ is chosen. The bias angle is changed to a new value every $T^* = n_0 T_0$ seconds where $T_0 = \frac{1}{f_0}$ is the fundamental period of f_p and m_p.

For the purposes of illustration, it is assumed that f_p and m_p have only fundamental components, and therefore it is assumed that $f_{s2}, f_{c2}, m_{s2}, m_{c2}$ are zero. Experimental results indicate that for zero bias angle, the mean values of f_p and m_p are zero. Therefore the vectors f_a, f_b, m_a, and m_b are selected as

$$f_a = (0, 5, 8), f_b = (20, 30, 36)$$

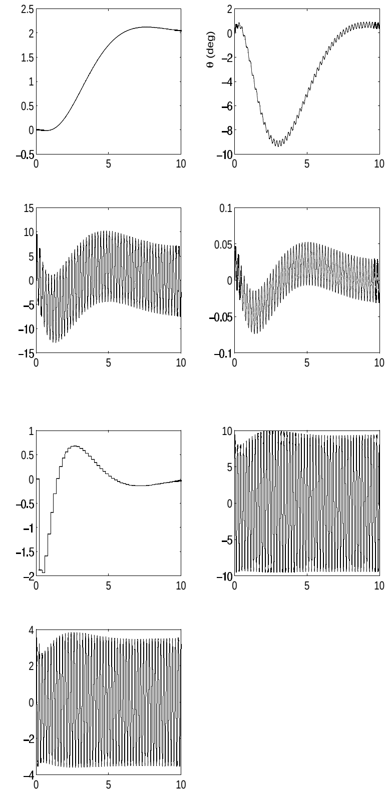

Figure 6: Feedback control: $z^* = 2$(m), $f_0 = 5$(Hz), sampling interval = 0.2 sec

$$m_a = (0, 1.5, 3.2), m_b = (10, 12, 9)$$

However, it is pointed out that the derived controller is effective even when the mean values are nonzero. The initial conditions and the terminal state are chosen as $x(0) = (0, 0, 0, 0)^T$ and $x^* = (0, 0, 2, 0)^T$ with $z^* = 2$ (m). Thus one desires to move to a depth of 2 (m).

Case 6.1 Closed-loop control: frequency f_0 = 5 Hz, $T^* = T_0$

The closed-loop system (3) including the discrete control law (26) is simulated. The frequency of oscillation is $f_0 = 5$ (Hz) and the sampling period is $T^* = T_0 = 0.2$ (sec). That is, the bias angle is updated every cycle. The simulated responses are shown in Fig. 6. A smooth regulation of the depth trajectory to the desired value of 2 (m) is accomplished. The response time is of the order of 10 seconds. The oscillatory normal force and moment are within 10 (N) and 4 (Nm), respectively. It is observed that the pitch angle response has oscillations of tiny amplitude superimposed over a smooth mean motion. It is pointed out that these tiny oscillations of the pitch angle persist even in the steady-state. However, it is interesting to note that this minor pitching motion causes no problem. The vehicle con-

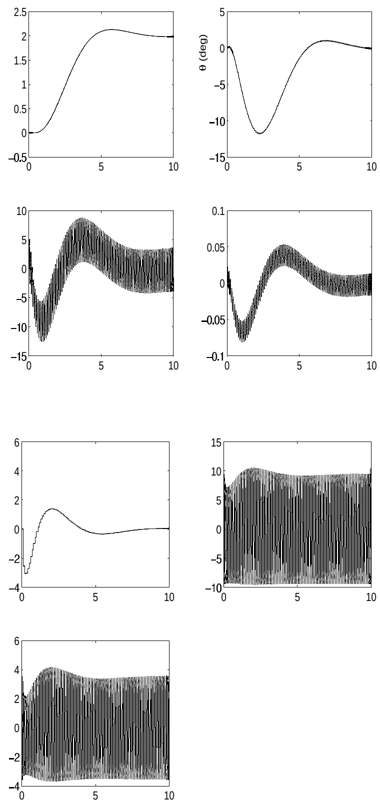

Figure 7: Feedback control: $z^* = 2$(m), $f_0 = 10$(Hz), sampling interval $= 0.1$ (sec)

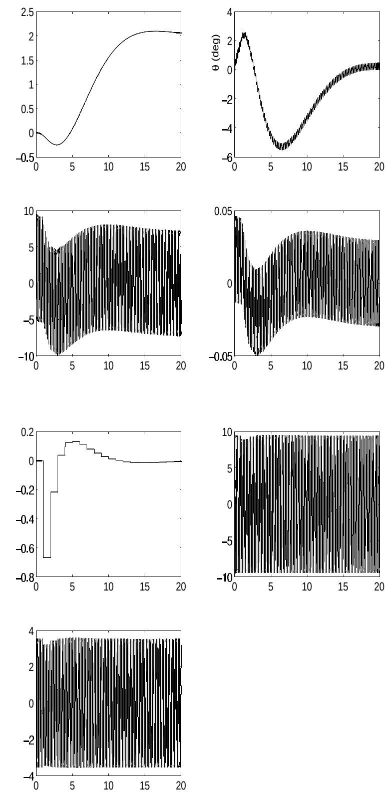

Figure 8: Feedback control: $z^* = 2$(m), $f_0 = 5$ (Hz), sampling interval $= 1$ (sec)

tinues to move horizontally and the perturbations in the depth trajectory between the sampling instants due to the pitching action of the vehicle are hardly noticeable. The piecewise constant bias angle remains within 2 (deg).

Case 6.2 Closed-loop control: $f_0 = 10$ (Hz), $T^* = T_0$

It is assumed that the fins are oscillating with a higher frequency 10 (Hz) (twice of that used in Case 6.1) and the sampling period is $T^* = T_0 = 0.1$ (Sec).

It is seen that precise control of the depth of the vehicle is obtained (Fig. 7) and compared to the Case 6.1, one has a smaller tracking error at $t = 10$ (sec). This is expected since the bias angle is updated at a faster rate compared to Case 6.1. The responses remain close to those of Case 6.1, and the fin force and moment have magnitudes of similar order. The bias angle magnitude is only slightly higher in this case. The tiny oscillations in the pitch trajectory observed for lower frequency in Fig. 7 have almost disappeared. Thus it seems that the choice of fins oscillating at higher frequencies is preferable.

Case 6.3 Closed-loop control: $f = 5$ (Hz), $T^* = 5T_0$ second

Here, the frequency of oscillation is retained at $f_0 = 5$ (Hz) similar to Case 6.1, but a slower sampling rate of value $T^* = 5T_0 = 1$ (sec) is assumed. Thus now unlike Case 6.1, the bias angle switches to new values at the interval of one second instead of 0.2 (sec). We observed that compared to Case 6.1, the response time (20 seconds) has almost doubled (Fig. 8). But the fin force and moment have magnitudes of similar order. It is seen that initially the depth trajectory has a slight overshoot in the wrong direction (upward motion) but recovers and dives down to attain the desired depth. Apparently, slower sampling rate has a detrimental effect on the maneuverability of the vehicle, but this may not be avoidable, especially when the actuators are slower.

7. Conclusion

The design of control systems for the dive plane maneuver using pectoral fins was considered. Pectoral fins have lead-lag, feathering and flapping modes of oscillations and have ability to produce maneuvering forces and moments which are functions of oscillation parameters (frequency, amplitude, bias angle and phase angle). The periodic forces and moments can be uniquely characterized by the associated Fourier coefficients. An open-loop control law was derived which determine a set of Fourier coefficients (i.e; fin forces and moment) for finite time maneuver of the vehicle in the depth plane. Besides the open-loop controller, a feedback control system was designed by utilizing periodically varying bias angle of the fins as control input. The closed-loop controller was designed using a discrete-time form of the model incorporating integral feedback. The complete open-loop and closed-loop systems were simulated for various types of dive-plane maneuvers which showed that using pectoral fins, one can perform precise and rapid maneuvers using the open-loop and feedback controllers.

8. Acknowledgment

This research was supported by the Office of Naval Research (ONR) (N0014-03-1-0459). Authors would like to thank Dr. Promode R. Bandyopadhyay, Program Manager, Office of Naval Research, for providing many useful suggestions for this research.

References

[1] A. Azuma, *The Bio-Kinetics of Flying and Swimming,* Springer-Verlag, New York, 1992.

[2] M. Sfakiotakis, D.M. Lane, and J.B.C. Davies, *"Review of Fish Swimming Modes for Aquatic Locomotion,"* IEEE Jl. Oceanic Engg., Vol.24, No. 2, April 1999, pp 237-252.

[3] P.R. Bandyopadhyay, J.M Castano, J.Q. Rice, R.B. Philips, W.H. Nedderman and W.K. Macy, *"Low-Speed Maneuvering Hydrodynamics of Fish and Small Underwater Vehicles,"* ASME Jl. Fluids Eng., Vol. 119, 1997, pp. 136-144

[4] G.S. Triantafyllou and M.S Triantafyllou, *"An Efficient Swimming Machine,"* Sci. Amer. 272:64-70

[5] C.B. Martin, F.S. Hover and M.S Triantafyllou, *"Maneuvering Performance Of A Rolling and Pitching Wing untethered Submersible Technology,"* Proceedings of the 12th International Symposium on UAVs.

[6] P.R. Bandyopadhyay, J.M Castano and J. Dick, *"Biologically-inspired bodies under surface waves- Part 1: Load Measurement,"* ASME Journal of Fluids Engineering, June 1999, Vol. 121, pp. 469-478

[7] P.R. Bandyopadhyay, S.N. Singh and F. Chockalingam, *"Biologically-inspired bodies under surface waves- Part 2: Theoretical control of maneuvering,"* ASME Journal of Fluids Engineering, June 1999, Vol. 121, pp. 479-487

[8] P.R. Bandyopadhyay, *"Maneuvering Hydrodynamics of Fish and Small Underwater Vehicles,"* Integ. And Comp. Biol., 42:102-117, 2002.

[9] I. Yamamoto, Y. Terada, T. Nagamutu and Y. Imaizumi *"Propulsion System with Flexible/Rigid Oscillating Fin,"* IEEE Jl. Oceanic Engg., Vol.20,No. 1, April 1995, pp 23-30.

[10] N. Kato *"Pectoral Fin Controllers,"* Neurotechnology for Biometric Robots, 2002

[11] N. Kato *"Performance in the Horizontal Plane of a Fish Robot with Mechanical Pectoral Fins,"* IEEE Jl. Oceanic Engg., Vol.25, No. 1, April 2000, pp 121-129.

[12] R. Mittal, Y. Utturkar and H.S. Udaykumar *"Computational Modeling and Analysis of Biometric Flight Mechanisms,"* AIAA 2002-0865

[13] R. Ramamurti, R. Lohner and W. Snadberg, *"Computation of the unsteady-flow past a tuna with caudal fin oscillation,"* Adv. Fluid Mech. Series, Vol 9, pp. 169-178, 1996

[14] J-S. Lee, C. Kim and O-H. Rho, *"The Modification of Airfoil Shape For Optimal Aerodynamic Performance On Flapping-Airfoil In Low-Reynolds Number Flow,"* AIAA 2003-421

[15] K.A. Harper, M.D. Berkemeier and S. Grace, *"Modeling the Dynamics of Spring-Driven Oscillating-Foil Propulsion,"* IEEE Jl. Oceanic Engg., Vol.23,No. 3, July 1998, pp 285-296.

[16] T. Kailath, *"Linear Systems,"* Prentice-Hall Inc., 1980

[17] C.T. Chen, *"Linear System Theory and Design,"* Oxford, 1999.

[18] K. Ogata, *"Discrete-Time Control Systems,"* Prentice-Hall Inc., 1987.